J Solid State Electrochem (2001) 5: 17–22

ORIGINAL PAPER

Frank Marken · Alastair N. Blythe · Jay D. Wadhawan
Richard G. Compton · Steven D. Bull · Robin T. Aplin
Stephen G. Davies

Voltammetry of electroactive liquid redox systems: anion insertion and chemical reactions in microdroplets of *para*-tetrakis(6-methoxyhexyl) phenylenediamine, *para*- and *meta*-tetrahexylphenylenediamine

Received: 15 November 1999 / Accepted: 2 December 1999

Abstract The effect of the structure of the organic precursor molecule on the electroinsertion of anions and on the formation of materials in the ionic liquid state is compared for three compounds, *para*-*N*, *N*, *N*′, *N*′-tetrahexylphenylenediamine (*p*-THPD), *meta*-*N*, *N*, *N*′, *N*′-tetrahexylphenylene diamine (*m*-THPD), and *para*-*N*, *N*, *N*′, *N*′-tetrakis(6-methoxyhexyl)phenylenediamine (*p*-TMHPD), by characterising their condensed phase voltammetric properties in aqueous media. The electrochemically driven anion insertion in *p*-THPD and *p*-TMHPD in the presence of ClO_4^-, F^-, Cl^-, Br^-, I^-, and SO_4^{2-} is shown to be extremely sensitive to structure. The introduction of the methoxy end groups in *p*-TMHPD causes (1) a considerable shift to more negative electroinsertion potentials, (2) a less stable response which upon continuous cycling decreases, and (3) considerably lower anion selectivity. For the insertion of sulfate, only *p*-TMHPD yields an electrochemical response which is shown to be consistent with insertion of the dianion SO_4^{2-}. The electrochemical oxidation of a deposit of *m*-THPD is accompanied by anion insertion and a chemical reaction step in an EC-type electrochemical process. The product of the chemical step is electrochemically active and results in a new reversible electroinsertion process. Starting materials and products of the microdroplet reactions are characterised by Maldi-TOF mass spectrometry and a reaction mechanism based on condensed phase polymerisation is proposed.

F. Marken (✉) · A.N. Blythe · J.D. Wadhawan
R.G. Compton
Physical & Theoretical Chemistry Laboratory,
Oxford University, South Parks Road,
Oxford OX1 3QZ, UK
e mail: Frank@physchem.ox.ac.uk
Tel.: +44-1865-275448; Fax: +44-1865-275410

S.D. Bull · R.T. Aplin · S.G. Davies
Dyson Perrins Laboratory, Oxford University,
South Parks Road, Oxford OX1 3QY, UK

Key words Ionic liquid · Microdroplet · Modified electrodes · Electroinsertion

Introduction

Recently, electroinsertion processes in solids, especially for the case of ion insertion into microcrystalline materials attached to electrode surfaces, have attracted considerable attention [1, 2] and mechanistic details have been shown to be complex [3, 4]. Similar electroinsertion processes can be studied for microdroplets of organic liquids, which after ion insertion give rise to the formation of ionic liquids.

Room temperature ionic liquids [5, 6] are interesting new materials which have been proposed as promising new reaction environments for catalytic [7, 8] and stoichiometric [9] chemical processes and as an alternative environmentally benign solvent system [10] in industrial processes. For electrochemical processes, ionic liquids may be regarded as well suited owing to their non-volatile and ion conducting nature [11, 12], making the use of supporting electrolyte unnecessary. Recent studies on electrochemical processes in ionic liquids focused on the redox chemistry of metal complexes [13], the reduction of protons [14], and their application in solar cell development [15].

A new area in ionic liquid redox chemistry involves modification of electrode surfaces with a thin layer or microdroplet deposit of an organic precursor material such as N^1-[4-(dihexylamino)phenyl]-N^1, N^4, N^4-trihexyl-1,4-phenylenediamine [16] or *para*-tetrahexylphenylenediamine [17, 18] (*p*-THPD, see Fig. 1) and redox cycling. In contrast to the use of thin organic solvent-based films [19, 20], the strategy for the generation of the ionic liquid is to deposit a suitable organic precursor molecule with extremely low solubility and a low tendency to solidify, and to electrochemically convert the precursor into an ionic liquid. The typical size of the microdroplets has been estimated based on AFM images

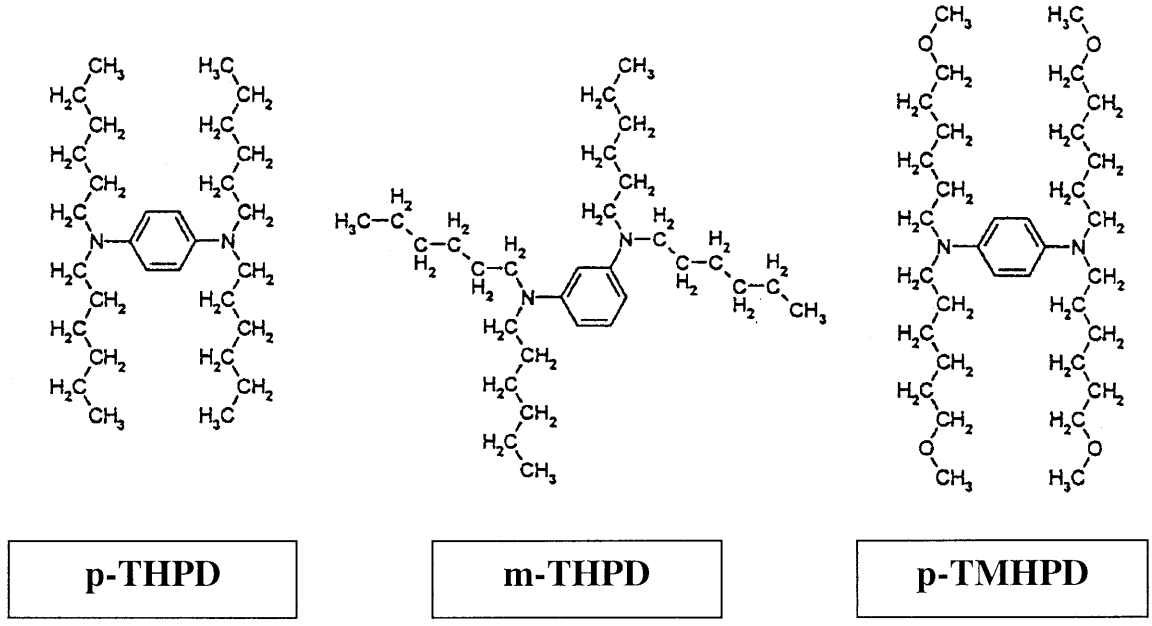

Fig. 1 Structures of *p*-THPD, *m*-THPD and *p*-PMHPD

and a simulation procedure to about 1 μm [21]. The deposit of *p*-THPD has been shown to undergo oxidation accompanied by anion insertion from the aqueous solution into the organic phase. This process is strongly dependent on the type and concentration of the anion present in the aqueous phase. It has been suggested [18] that the structure of the organic material deposited in form of microdroplets at the electrode surface strongly affects the interaction with the anion and that selectivity may be achieved by tailoring the structure for a specific ion. Redox-switchable ionic liquids are of potential importance in applications requiring ion conduction and for ion separation.

In this study the effects of changing the molecular structure of the organic precursor are studied for the case of a change in the side chain, *para*-tetrakis-(6-methoxyhexyl)phenylenediamine (*p*-TMHPD), and for the case of an isomer, *meta*-tetrahexylphenylene diamine (*m*-THPD). Dramatic changes in the voltammetric characteristic for both types of structural changes are observed and interpreted in terms of a change in anion-organic substrate interaction, possible water co-insertion, and chemical reaction steps leading to an unexpected polymerisation process in the microdroplet environment. Results are supported by Maldi-TOF MS analysis of the starting materials and products of the microdroplet reactions at the electrode aqueous solvent (electrolyte) interface.

Experimental

Chemical reagents

Aqueous electrolyte solutions have been prepared with NaF, NaCl, NaBr, KI (Aldrich), Li_2SO_4, K_2SO_4, and $NaClO_4$ (BDH). Chemical reagents were of analytical or the purest commercially available grade. De-ionised water was taken from an Elgastat filter system (Elga, Bucks, UK) and had a resistivity of not less than 18 M Ωcm.

p-THPD was prepared following a literature procedure [17]. The synthesis of *p*-TMHPD and *m*-THPD followed the same strategy. These materials were obtained in pure form after column chromatography with the following spectroscopic characteristics. *p*-TMHPD: ^{1}H NMR ($CDCl_3/C_7D_8$ [1:4]) 1.20 (16H, b); 1.48 (16H, b); 3.05 (8H, b, 4 × CH_2 N); 3.14 (12H, s, 4 × OMe); 3.18 (8H, t, 4 × CH_2OMe); 7.05 (4H, s, 4 × ArH); HRMS (M + 1) calc. for $C_{34}H_{65}N_2O_4$ 565.4944, found 565.4941. *m*-THPD: ^{1}H NMR ($CDCl_3$) 0.91 (12H, bt, 4 × Me); 1.31 (24H, b, 4 × $(CH_2)_3$); 1.63 (8H, b, 4 × CH_2); 3.23 (8H, t, 4 × CH_2 N); 5.92 (1H, s, ArH); 6.02 (2H, d, 7 Hz, 2 × ArH); 7.02 (1H, t, ArH); HRMS (M + 1) calc. for $C_{30}H_{57}N_2$ 445.4522, found 445.4518.

Instrumentation

Electrochemical experiments were conducted with a PGSTAT20 Autolab system (Ecochemie, Netherlands) in a conventional three-electrode cell. The electrodes used were a platinum gauze as the counter electrode and a saturated calomel electrode (Radiometer, Copenhagen) as the reference. The working electrode was a 4.9 mm diameter basal plane pyrolytic graphite disc mounted in a Teflon holder. Before and after electrochemical experiments the electrode surface was renewed by polishing on a fine carborundum paper. The deposition of microdroplets of organic materials was achieved by solvent evaporation using a 0.1 mM solution of the organic precursor in acetonitrile. Unless otherwise stated, experiments have been undertaken at 20 ± 2 °C.

Results and discussion

Electrochemically induced ion insertion in *p*-THPD

Microdroplet deposits of *p*-THPD are known [17] to undergo reversible anion insertion upon oxidation in suitable aqueous electrolyte media. In Fig. 2a the first seven cycles of a cyclic voltammogram are shown for *p*-THPD deposited on a basal plane pyrolytic graphite

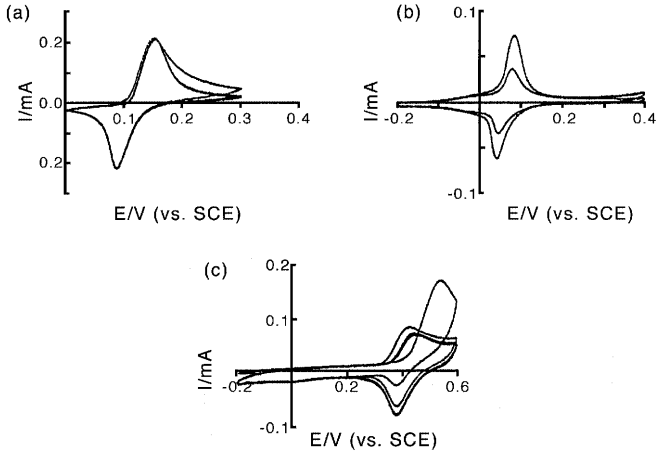

Fig. 2 Cyclic voltammograms recorded at 100 mV s^{-1} showing **a** the first seven scans for 6.8×10^{-9} moles *p*-THPD, **b** the first and eighth scans for 9.0×10^{-9} moles *p*-TMHPD, and **c** the first five scans for 11.3×10^{-9} moles *m*-THPD deposited by solvent evaporation onto a 4.9 mm diameter basal plane pyrolytic graphite electrode and immersed in aqueous 0.1 M $NaClO_4$

electrode and immersed in aqueous 0.1 M $NaClO_4$. Only the first reversible redox process at $E_{mid,P1} = 0.13$ V vs. SCE is shown. Formally the process, which involves electron transfer between deposit and the electrode accompanied by anion insertion and expulsion, may be described by Eq. 1:

$$p\text{-THPD}_{oil} + ClO_{4\,aq}^{-} \rightleftharpoons [p\text{-THPD}^{+}ClO_4^{-}]_{oil} + e^{-} \qquad (1)$$

It can be seen in Fig. 2a that after the initial potential cycle the system becomes stable and no significant change in the voltammetric response is detected over several cycles. Beyond that, in earlier work [17] the effect of the amount of deposit on the electrode surface has been studied, and it has been shown that the process is Nernstian in the sense that the mid-potential, E_{mid}, shows an approximately 59 mV shift per decade change of the concentration of $NaClO_4$ (for 0.002 M < $[ClO_4^-]$ < 1.0 M) in the aqueous solution phase.

In order to study and compare the electroinsertion process in more detail, aqueous 0.1 M solutions of the halides F^-, Cl^-, Br^-, and I^- were used as supporting electrolytes. Figure 3a–d show multicycle voltammograms recorded over a potential range from −0.2 to +0.4 V vs. SCE for 5.3×10^{-9} moles of *p*-THPD (2.3 μg) deposited on a basal plane pyrolytic graphite electrode. The oxidation process can be seen to be strongly dependent on the type of anion present in the aqueous phase. For F^-, only a very weak response at 0.24 V vs. SCE is detected. For Cl^-, Br^-, and I^-, a systematic trend for electroinsertion at more negative potential depending on the size or hydrophobicity can be observed (see Fig. 3 and Table 1).

The electroinsertion of Cl^- occurs just outside of the potential range (not shown) and it has been reported before [17] that the shape of the oxidation and re-reduction responses is complex and not reversible. A

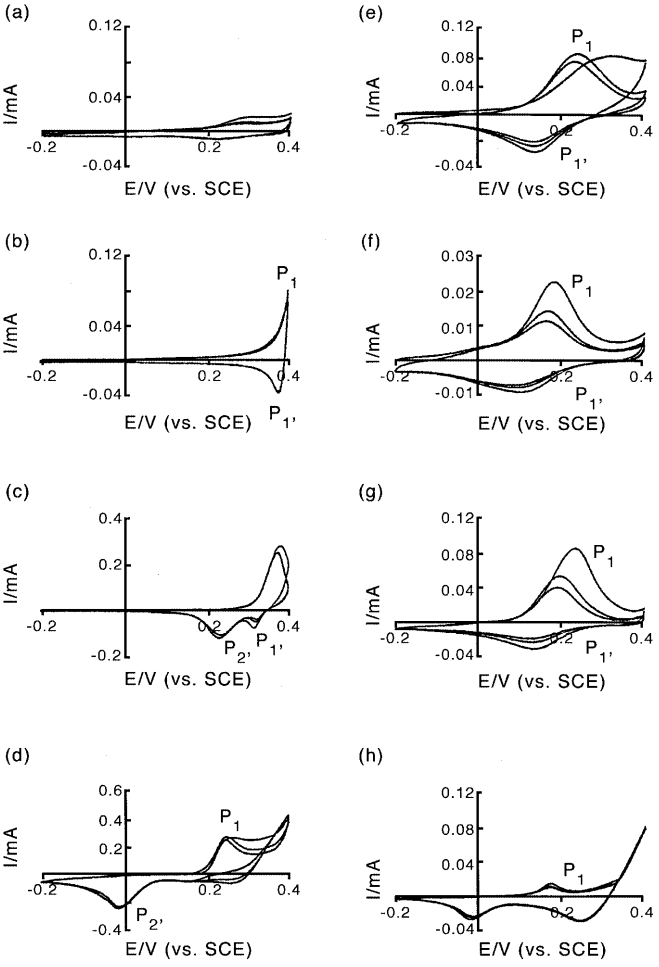

Fig. 3 Cyclic voltammograms (first three scans) recorded at 100 mV s^{-1} for the oxidation of 5.3×10^{-9} moles *p*-THPD deposited by solvent evaporation onto a 4.9 mm diameter basal plane pyrolytic graphite electrode immersed in aqueous 0.1 M **a** NaF, **b** NaCl, **c** NaBr, and **d** KI and for the oxidation of 3.6×10^{-9} moles *p*-TMHPD immersed in aqueous **e** NaF, **f** NaCl, **g** NaBr, and **h** KI

second re-reduction peak (not shown) similar to that observed for Br^- (see Fig. 3c, P_1 and P_2, Table 1) is detected when the potential is scanned more positive before reversing the scan direction. This second re-reduction for Cl^- and Br^- has to be attributed to a structural or composition change after oxidation. Two plausible explanations for the observed voltammetric characteristic are (1) a solidification process and (2) the rapid co-insertion of water followed by a slower equilibration which is accompanied by loss of water back into the aqueous phase.

It is interesting to note that heating the electrochemical cell to 40 °C causes the second response, P_2, to disappear and only P_1 is observed as a fully chemically reversible response. This observation rules out any irreversible chemical reaction steps. At elevated temperature the structural or composition change seems not to occur any more and only a simple reversible redox process is observed. The processes P_1 and P_2 may be

Table 1 Cyclic voltammetric data for the oxidation of *p*-THPD and *p*-TMHPD deposited onto a basal plane pyrolytic graphite electrode and immersed in 0.1 M aqueous electrolyte solution (scan rate 0.1 V s^{-1}, $T = 20$ °C)

	p-THPD				*p*-TMHPD			
	E_{P1}/ (V vs.SCE)	$E_{P1'}$/ (V vs. SCE)	$E_{P2'}$/ (V vs. SCE)	$E_{mid,P1}$/ (V vs. SCE)	E_{P1}/ (V vs. SCE)	$E_{P1'}$/ (V vs. SCE)	$E_{P2'}$/ (V vs. SCE)	$E_{mid,P1}$/ (V vs. SCE)
ClO_4^-	0.17	0.10	–	0.13	0.08	0.04	–	0.06
F^-	–	–	–	–	0.23	0.15	–	0.19
Cl^-	0.44	0.38	–	0.41	0.19	0.11	–	0.15
Br^-	0.38	0.32	0.23	0.35	0.24	0.15	–	0.19
I^-	0.25	–	−0.01	–	0.18	–	−0.02	–

described by Eq. 2:

$$THPD_{oil} + X^-_{aq} \rightleftharpoons [THPD^+X^-]_{oil,A} + e^- \quad (2a)$$

$$[THPD^+X^-]_{oil,A} \rightleftharpoons [THPD^+X^-]_{oil,B} \quad (2b)$$

$$[THPD^+X^-]_{oil,B} + e^- \rightleftharpoons THPD_{oil} + X^-_{aq} \quad (2c)$$

Both a structural change due to phase transition/solidification or due to co-insertion of water and a transition (Eq. 2b) accompanied by water release are possible. A solidification process would explain the voltammetric characteristics but is not consistent with observations made with other types of anions such as ClO_4^- and PF_6^- [18]. However, the co-insertion of water during electroinsertion of halide in the process P_1 on the other hand, is very likely and may explain the observed voltammetric characteristics. Furthermore, the proposed co-insertion of water is consistent with observations made for the oxidation of *p*-TMHPD (vide infra).

The electroinsertion of Br^- during oxidation of *p*-THPD (Fig. 3c) is very closely related to the process in the presence of Cl^-. Reversing the potential in the foot of process P_1 causes $P_{1'}$ to dominate over $P_{2'}$ and a gentle temperature increase to 40 °C causes process $P_{2'}$ to disappear. That is, the electroinsertion of Br^- also becomes fully chemically reversible at slightly elevated temperatures. The electroinsertion and expulsion of I^- into microdroplets of *p*-THPD deposited on a basal plane pyrolytic graphite electrode (Fig. 3d) results in a voltammetric response with a wide potential gap between oxidation and reduction response (see Table 1). The response corresponding to $P_{1'}$ is not observed under these conditions, even at 40 °C. The integration of the charge under the peak P_1 gives a result consistent with a one-electron oxidation of *p*-THPD. Therefore the formation of the I_3^- instead of the I^- ionic liquid can be ruled out and the process may again be described by the reaction scheme given in Eq. 2. However, for the iodide insertion process the chemical step, Eq. 2b, appears to be faster. The release of water from the ionic liquid could be considerably increased in the case of the less hydrophilic I^- anion.

The observation that during electroinsertion the "high-energy modification", $[THPD^+X^-]_{oil,A}$, is formed which then rapidly relaxes to the low-energy form, $[THPD^+X^-]_{oil,B}$, has interesting implications for the insertion mechanism, at least for the case of the halide electroinsertion process. Why is the formation of $[THPD^+X^-]_{oil,B}$ not possible directly? There appears to be a kinetic barrier, which stops the direct insertion of X^- and which favours water incorporation and the formation of the intermediate $[THPD^+X^-]_{oil,A}$. Instead, by anions crossing the aqueous solutionorganic phase boundary (Fig. 4a) the process might be more appropriately described as formation of the product directly from the "wet" surface phase via convective transport (Fig. 4b). The latter Marangoni-type transport mechanism [22] is not inconsistent with observations made by microscopy [17] and could be considerably faster compard to only diffusion [21]. More importantly, the composition of the product formed in this process may be determined by the surface composition of the oil dropletaqueous electrolyte interface. Therefore compositional changes upon formation of the product are possible.

Electrochemically induced ion insertion in *p*-TMHPD

The structure of the organic precursor molecule can be shown to have a considerable effect on the nature of the

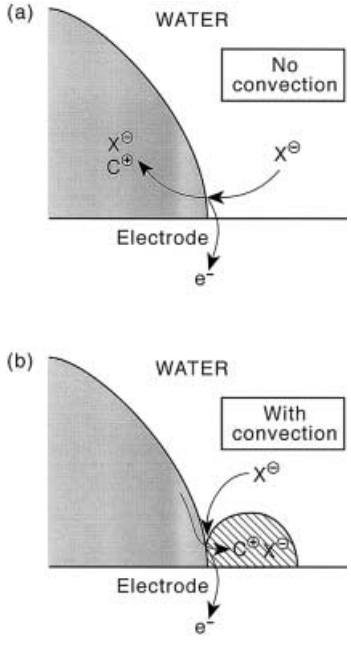

Fig. 4 Schematic drawing indicating two mechanistic pathways, **a** without and **b** with convection, for the conversion of droplets of THPD to $THPD^+X^-$

anion electroinsertion process. In Fig. 2b the oxidation of 3.6×10^{-9} moles of *p*-TMHPD (1.6 μg) deposited in the form of microdroplets onto a basal plane pyrolytic graphite electrode and immersed in aqueous 0.1 M $NaClO_4$ is shown. The mid-potential, $E_{mid} = 0.06$ V vs. SCE, can be seen to be shifted to more negative potentials compared to the process observed for *p*-THPD, $E_{mid} = 0.13$ V vs. SCE (Fig. 2a). This shift in potential is surprising because the molecular structure has been only slightly modified far away from the redox-active part of the molecule. This indicates that the uptake of anions from the solution phase is a more facile process, presumably owing to the presence of the more polar methoxy end groups. Further, from the difference between the first and the eighth cycle (Fig. 2b) it can be seen that the deposit is less stable and material is likely to be lost into the solution phase during the course of redox cycling.

In Fig. 3e–h it can be seen that the oxidation of 3.6×10^{-9} moles *p*-TMHPD deposited onto a basal plane pyrolytic graphite electrode gives well-defined voltammetric responses in the presence of F^-, Cl^-, Br^-, and I^-. The voltammetric responses observed for F^-, Cl^-, and Br^- are remarkably similar and always occur at potentials negative to those observed for the corresponding *p*-THPD processes (Fig. 2a–c, Table 1). The electroinsertion of anions into *p*-TMHPD appears therefore to be much more facile and essentially non-selective. For F^-, Cl^-, and Br^- the observed voltammetric response is attributed to the process P_1. The lack of selectivity towards specific anions as well as the partial loss of material in the oxidised state strongly suggest substantial incorporation of water into the product formed in this process. Only for the case of I^- is insertion process P_2 detected, presumably owing to the more favourable release of water from the more hydrophobic iodide-containing ionic liquid.

It has been reported in previous work [17] that doubly charged anions are not able to undergo electroinsertion into the organic microdroplet phase when *p*-THPD is used. The comparison of *p*-THPD and *p*-TMHPD shown in Fig. 5 clearly demonstrates the difference in selectivity. In the potential range from −0.2 to 0.4 V vs. SCE, no electroinsertion into *p*-THPD occurs but welldefined responses are observed for *p*-TMHPD, again in the same potential range where the monoanionic electroinsertion processes have been observed (see Table 1). The cation present in the aqueous electrolyte solution, Li^+ or K^+, can be seen to have no significant influence on the voltammetric responses and the question arises whether proton uptake accompanies the electroinsertion of sulfate. The pH dependence of the voltammetric response has been investigated over a wide pH range (see Fig. 6) and the observed peak potential for the oxidation process, E_{p1}, has been found to remain essentially constant. Therefore the process is proposed to be associated with the electroinsertion of SO_4^{2-} (Eq. 3):

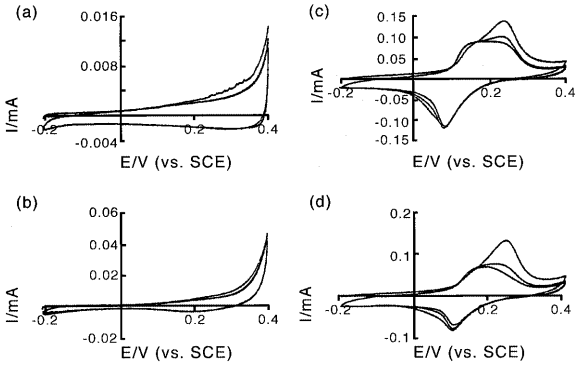

Fig. 5 Cyclic voltammograms (first three scans) recorded at 100 mV s^{-1} for the oxidation of 5.3×10^{-9} moles *p*-THPD deposited by solvent evaporation onto a 4.9 mm diameter basal plane pyrolytic graphite electrode immersed in aqueous 0.1 M **a** Li_2SO_4 and **b** K_2SO_4 and for the oxidation of 3.6×10^{-9} moles *p*-TMHPD immersed in aqueous 0.1 M **c** Li_2SO_4 and **d** K_2SO_4

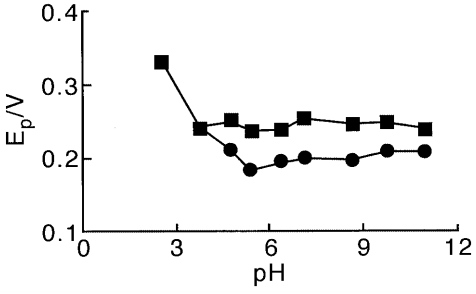

Fig. 6 Peak positions in V vs. SCE for the first (*squares*) and the fourth (*circles*) cyclic voltammtric scans at 100 mV s^{-1} for the oxidation of 3.6×10^{-9} moles of *p*-TMHPD deposited on a 4.9 mm diameter basal plane pyrolytic graphite electrode and immersed in aqueous 0.1 M potassium sulfate as a function of pH

$$2[\mathrm{TMHPD}]_{oil} + {SO_4^{2-}}_{aq} \rightleftharpoons [(\mathrm{TMHPD}^+)_2 SO_4^{2-}]_{oil} + 2e^- \quad (3)$$

Electrochemically induced ion insertion in *m*-THPD

By introducing a structural change from the *para*- to *meta*-tetrahexylphenylenediamine, another novel feature in the voltammetric oxidation response can be detected. In Fig. 2c it can be seen that the strong voltammetric peak at $E_{P,ox} = 0.54$ V vs. SCE in the first cycle is followed by a rather weak re-reduction response. In the following potential cycles a new and reversible process is observed at $E_{P,ox} = 0.44$ V vs. SCE and $E_{P,red} = 0.38$ V vs. SCE. The process is associated with a chemical step yielding a new material with a slightly more negative oxidation potential. Therefore a coupling or dimerisation process may be proposed (vide infra) to explain the voltammetric characteristics.

In order to further study the nature of the product formed after the chemical reaction step, microgram

Table 2 Data from Maldi-TOF mass spectroscopy of *p*-THPD, *p*-TMHPD, and *m*-THPD deposited on a basal plane pyrolytic graphite electrode (1) untreated and (2) after immersion in 0.1 M $NaClO_4$ and applying a potential of 0.3 V vs. SCE for *p*-THPD, *p*-TMHPD, and 0.6 V vs. SCE for *m*-THPD

	Mol. weight (g/mol)	(1) Before oxidation mol.ion (*m*/*z*)	(2) After oxidation mol.ion (*m*/*z*)
p-THPD	444	444.9 $[M]^+$	444.9 $[M]^+$
p-TMHPD	564	564.7 $[M]^+$	564.7 $[M]^+$
m-THPD	444	441.6 $[M]^+$	441.5 $[M]^+$
			800.8 $[M_2\text{-hexyl}]^+$
			886.0 $[M_2]^+$
			1244.4 $[M_3\text{-hexyl}]^+$
			1330.5 $[M_3]^+$
			1688.9 $[M_4\text{-hexyl}]^+$
			1774.1 $[M_4]^+$

quantities of the starting material as well as products deposited onto basal plane pyrolytic graphite were examined by Maldi-TOF mass spectrometry. In Table 2, selected data are summarised. It can be seen that the chemical reversibility of the *p*-THPD and *p*-TMHPD redox processes is reflected by the corresponding molecular ion signals. However, for *m*-THPD a considerable change occurs and the dimeric as well as oligomeric molecular ions are detected. A series of signals detected by mass spectrometry can be interpreted in terms of oligomers (up to the tetramer) and the corresponding molecular ions after loss of a hexyl side chain (Table 2). Therefore the overall process for the oxidation of *m*-THPD may be proposed to follow the following reaction pathway (Eq. 4):

$$[m\text{-THPD}]_{oil} + ClO_4^- \rightleftharpoons [m\text{-THPD}^+ClO_4^-]_{oil} + e^- \quad (4a)$$

$$2[m\text{-THPD}^+ClO_4^-]_{oil} \rightleftharpoons [(m\text{-THPD})_2]_{oil} + 2H^+ + 2ClO_4^- \quad (4b)$$

$$[(m\text{-THPD})_2]_{oil} + ClO_4^- \rightarrow [(m\text{-THPD})_2^+ClO_4^-]_{oil} + e^- \quad (4c)$$

This reaction scheme explains the presence of a very small re-reduction response on the first potential cycle. The coupling process directly yields the reduced form of the redox system and protons, which are expelled into the aqueous solution phase. Then, in the following potential cycles the new reversible voltammetric response develops with a smaller peak current. The coincident potential ranges for the oxidation of the two materials $[m\text{-THPD}]_{oil}$ and $[(m\text{-THPD})_2]_{oil}$ allow the processes to be coupled and to go to completion after 2–3 potential cycles.

Additionally, it can be concluded that also the formation of oligomeric products is possible. This finding is consistent with the ''condensed phase'' electropolymerisation of *m*-THPD upon oxidation and perchlorate anion insertion. This novel type of electropolymerisation process is based on a droplet deposit of organic oil rather than on electrodeposition and could have interesting applications, e.g. for the formation of structured polymer deposits.

Conclusions

It has been shown that the structure of the organic precursor molecule used for the electrochemical formation of ionic liquid materials deposited on basal plane pyrolytic graphite electrode surfaces is of key importance. The introduction of methoxy end groups not only caused a considerable shift in the potential at which electroinsertion occurs, it also caused the loss of the selectivity of the electroinsertion process towards specific anions. Further, the *m*-THPD isomer has been shown to undergo electropolymerisation in the microdroplet environment. Mechanistic details for this process as well as for water co-insertion processes are the subject of further investigation.

Acknowledgements F.M. thanks the Royal Society for a University Research Fellowship and New College, Oxford, for a Stipendiary Lectureship.

References

1. Scholz F, Lange B (1994) Chem Soc Rev 23: 341
2. Bond AM, Marken F (1994) J Electroanal Chem 372: 125
3. Bond AM, Fletcher S, Marken F, Shaw SJ, Symons PG (1996) J Chem Soc Faraday Trans 92: 3925
4. Suarez MF, Marken F, Compton RG, Bond AB, Miao W, Raston CL (1999) J Phys Chem B 103: 5637
5. Suarez PAZ, Einloft S, Dullius JEL, de Souza RF, Dupont J (1998) J Chim Phys 95: 1626
6. Bradley D (1999) Chem Ind (London) 86
7. Suarez PAZ, Rosa NT, Einloft S, de Souza RF, Dick YP (1998) Polym Bull 41: 175
8. Earle MJ, McCormac PB, Seddon KR (1998) J Chem Soc Chem Commun 2245
9. Adams CJ, Earle MJ, Seddon KR (1999) J Chem Soc Chem Commun 1043
10. Seddon KR (1997) J Chem Technol Biotechnol 68: 351
11. Osteryoung RA, Gale RJ, Robinson J, Linga H, Cheek G (1981) J Electrochem Soc 128: C79
12. Bockris JO'M, Reddy AKN (1998) Modern electrochemistry 1: ionics. Plenum Press, London
13. Sun IW, Ward EH, Hussey CL, Seddon KR, Turp JE (1987) Inorg Chem 26: 2141
14. Campbell JLE, Johnson KE (1995) J Am Chem Soc 117: 779
15. Bonhote P, Dias AP, Papageorgiou N, Kalyanasundaram, Grätzel M (1996) Inorg Chem 35: 1168
16. Marken F, Blythe A, Compton RG, Bull SD, Davies SG (1999) J Chem Soc Chem Commun 1823
17. Marken F, Webster RD, Bull SD, Davies SG (1997) J Electroanal Chem 437: 209
18. Marken F, Compton RG, Goeting CH, Foord JS, Bull SD, Davies SG (1998) Electroanalysis 10: 821
19. Shi CN, Anson FC (1999) J Phys Chem B 103: 6283
20. Shi CN, Anson FC (1998) Anal Chem 70: 3114
21. Ball JC, Marken F, Fulian Q, Wadhawan JD, Blythe AN, Schröder U, Compton RG, Bull SD, Davies SG Electroanalysis (in press)
22. Velarde MG (1998) Philos Trans R Soc London Ser A 356: 829